CrossMark
←click for updates

Mutational Analysis of Quinolone Resistance Protein QnrVC7 Provides Novel Insights into the Structure-Activity Relationship of Qnr Proteins

Kathy Hiu Laam Po,[a,b] Edward Wai Chi Chan,[a,b] Sheng Chen[a,b]

Shenzhen Key Lab for Food Biological Safety Control, Food Safety and Technology Research Center, Hong Kong Polytechnic University Shenzhen Research Institute, Shenzhen, People's Republic of China[a]; State Key Lab of Chirosciences, Department of Applied Biology and Chemical Technology, The Hong Kong Polytechnic University, Hung Hom, Kowloon, Hong Kong,[b] People's Republic of China

This study assessed the functional importance of residues located at the i^{-2} position of face 4 of the tandem repeat loops of the quinolone resistance protein QnrVC7 through mutagenesis studies. The i^{-2} position of face 4 on different coils required residues with different natures. Some substitutions reduced the protective activity of QnrVC7, while some of them increased it. These findings advanced our understanding on the detailed structural organization and functional requirements of Qnr proteins.

Qnr proteins are pentapeptide repeat proteins (PRPs) that contribute to reduced susceptibility to quinolones in Gram-negative bacteria [1]. Knowledge regarding the crystal structure of QnrB1, which was reported previously [1], indicates that the protein comprises 10 tandem-repeated loops, with each containing 4 faces and each face represented by the i, i^{+1}, i^{+2}, i^{-1}, and i^{-2} positions. This class of proteins exhibits structural similarity to double-stranded DNA, with 5 amino acids forming a tandem-repeat unit, which in turn folds into a right-handed quadrilateral β-helix. The Qnr proteins confer reduced susceptibility to quinolones through competition with DNA in binding to DNA gyrase and topoisomerase IV, thereby preventing DNA breakage due to quinolone binding [2, 3]. To date, a total of 6 classes of Qnr proteins, namely, QnrA, QnrB, QnrC, QnrD, QnrS, and QnrVC, have been discovered, among which QnrB is the most prevalent subtype and can be further subdivided into 80 variants [4–8]. Mutational analyses of QnrA, QnrB, QnrC, and QnrS have identified several conserved residues that play an important role in the stabilization of the Qnr protein structure [1, 3, 9–11], most of which being located at the i and i^{-2} positions, as defined by Vetting et al. [1]. In addition, the C terminus of Qnr proteins, which has been suggested to be responsible for the formation of dimers, was found to be critical for Qnr function [3]. Two conservative extra loops of QnrB1 were also shown to be critical for Qnr protective activity, as the deletion of these loops dramatically affected its protective function [1]. Recently, our group identified a novel chromosomally encoded Qnr variant, QnrVC7, which exhibited lower protection activity than that of other Qnr proteins, such as QnrVC5 and QnrVC6, and other Qnr proteins. Sequence comparison and mutational analysis showed that amino acid T^{152}, located at the i^{-2} position on face 4, was responsible for the reduced protective activity of QnrVC7 [12]. This study extended the characterization to all residues located at the i^{-2} position of face 4 to elucidate the structure-activity relationships of QnrVC7 and other Qnr proteins.

The entire coding region of QnrVC7 was amplified using chromosomal DNA from *Vibrio cholerae* V122 as the template, ligated to pCR2.1 vector, and then transformed into *Escherichia coli* strain TG1 to construct pCR2.1-*qnrVC7* [12]. Site-directed mutagenesis using the GeneArt site-directed mutagenesis system (Invitrogen)

was performed on all residues located at the i^{-2} position of face 4, including A^{36}, S^{62}, A^{82}, A^{102}, A^{152}, Q^{132}, and C^{172} (Fig. 1A and B). *E. coli* TG1 isolates carrying different *qnrVC7* mutations were assayed, upon induction by 1 mM isopropyl-β-D-thiogalactopyranoside (IPTG), for their quinolone susceptibilities by the broth microdilution method, according to the Clinical and Laboratory Standards Institute (CLSI) guidelines [13], to determine the effect of amino acid substitutions of each residue on the protective effect of the *qnrVC7* gene product. To better understand the mutational analysis data, the structure of QnrVC was modeled using QnrB1(2XTW) as the template, through the use of SWISS-MODEL, and the final structure was refined by PyMOL, as previously described [14]. Structural analysis showed that coils 1 to 4 and 5 to 7 of QnrVC7 were arranged in the form of relatively tight and well-organized stacks, with similar space between the two stacks, whereas stacks between coils 4 and 5 and 7 and 8 were in a less-organized format, with wider spaces between the stacks (Fig. 1B). On the other hand, residues A^{36}, S^{62}, A^{82}, and A^{102} were found to be located at the i^{-2} position of face 4 of coils 1 to 4 of QnrVC7, respectively.

The amino acid substitutions $A^{36}T$ and $A^{36}G$ did not exhibit apparent effects on QnrVC7 protective activity, according to the ciprofloxacin MIC data, yet replacement with larger-chain residues, as exemplified by the $A^{36}L$ and $A^{36}D$ changes, completely abolished the protective function of QnrVC7 (Table 1). Similarly, the $S^{62}A$ substitution exhibited no effect, and the $S^{62}T$ amino acid change was found to display only minor effects on the protective activity of QnrVC7; however, other substitutions, such as $S^{62}G$, $S^{62}L$, and $S^{62}D$, completely abolished the protective activity of

(A)

```
i⁻² i⁻¹ i i⁺¹ i⁺²   i⁻² i⁻¹ i i⁺¹ i⁺²   i⁻² i⁻¹ i i⁺¹ i⁺²   i⁻² i⁻¹ i i⁺¹ i⁺²
  M D K T D           Q L Y V Q           A D F S H           Q D L S G        20
  Q Y F K N           C K F F C           C S F K R           A N L R D        40
  T Q F V D           C S F I E           R G E L E G         C D F S Y        61
  S D L R D           A S F K N           C S L S M           S Y F K G        81
  A N C F G           I E F R E           C D L K G           A N F A Q       101
  A S F M N           Q V S N R           M Y F C S           A Y I T G       121
  C N L S Y           A N F E R           Q C I E K           C D L F E       141
  N R W I G           A N L S G           T S F K E           S D L S R       161
  G V F S E           G C W S Q           C R L Q G           C D L S H       181
  S E L Y G           L D P R K           V D L T G           V K I C S       201
  W Q Q E Q           L L E Q L           G L I V V           P D             218
```
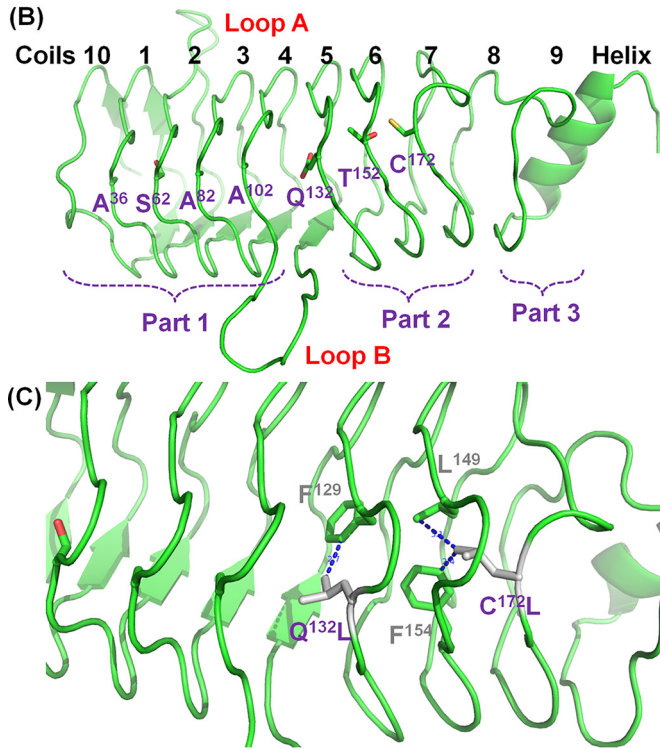
(B)

(C)

FIG 1 Amino acid sequence and structural representation of QnrVC7 and specific mutant proteins. (A) Tabular array of QnrV7 amino acids grouped by pentapeptide repeats, with coils along the vertical axis and faces along the horizontal axis; i^{-2} residues characterized in this study are in bold. (B) Overall structure of QnrVC7 and its organization. The sites at the i^{-2} position of face 4 are indicated in purple. (C) Amino acid substitutions that led to an increase in protective activity of QnrVC7. The potential hydrophobic interactions that may enhance the stability of QnrVC7 are indicated in gray and purple.

of other faces in QnrVC and other Qnr proteins, such as QnrB1 (3, 9, 12).

It was shown in our previous study that QnrVC7 differed from QnrVC5, QnrVC6, and other Qnr proteins by having a threonine at the 152 site (12). In this work, a mutation causing the $T^{152}A$ change was found to effectively convert QnrVC7 to other Qnr

TABLE 1 Ciprofloxacin MICs of Qnr-producing *E. coli* TG1 mutants

Protein or mutation type, residue	Strain ID[a]	CIP MIC (µg/ml)[b]
Control	TG1(pCR2.1-*qnrVC5*)	0.25
	TG1(pCR2.1-*qnrVC7*)	0.06
	TG1(pCR2.1)	0.015
	TG1	0.015
QnrVC7, A^{36}	TG1(pCR2.1-*qnrVC7*-A^{36}T)	0.06
	TG1(pCR2.1-*qnrVC7*-A^{36}G)	0.06
	TG1(pCR2.1-*qnrVC7*-A^{36}L)	0.015
	TG1(pCR2.1-*qnrVC7*-A^{36}D)	0.015
QnrVC7, S^{62}	TG1(pCR2.1-*qnrVC7*-S^{62}T)	0.03
	TG1(pCR2.1-*qnrVC7*-S^{62}G)	0.015
	TG1(pCR2.1-*qnrVC7*-S^{62}L)	0.015
	TG1(pCR2.1-*qnrVC7*-S^{62}D)	0.015
	TG1(pCR2.1-*qnrVC7*-S^{62}A)	0.06
QnrVC7, A^{82}	TG1(pCR2.1-*qnrVC7*-A^{82}T)	0.015
	TG1(pCR2.1-*qnrVC7*-A^{82}G)	0.015
	TG1(pCR2.1-*qnrVC7*-A^{82}L)	0.015
	TG1(pCR2.1-*qnrVC7*-A^{82}D)	0.015
	TG1(pCR2.1-*qnrVC7*-A^{82}I)	0.015
	TG1(pCR2.1-*qnrVC7*-A^{82}S)	0.03
QnrVC7, A^{102}	TG1(pCR2.1-*qnrVC7*-A^{102}T)	0.015
	TG1(pCR2.1-*qnrVC7*-A^{102}G)	0.015
	TG1(pCR2.1-*qnrVC7*-A^{102}L)	0.015
	TG1(pCR2.1-*qnrVC7*-A^{102}D)	0.015
QnrVC7, Q^{132}	TG1(pCR2.1-*qnrVC7*-Q^{132}T)	0.06
	TG1(pCR2.1-*qnrVC7*-Q^{132}G)	0.06
	TG1(pCR2.1-*qnrVC7*-Q^{132}L)	0.25
	TG1(pCR2.1-*qnrVC7*-Q^{132}D)	0.015
	TG1(pCR2.1-*qnrVC7*-Q^{132}A)	0.125
QnrVC7, T^{152}	TG1(pCR2.1-*qnrVC7*-T^{152}G)	0.015
	TG1(pCR2.1-*qnrVC7*-T^{152}L)	0.015
	TG1(pCR2.1-*qnrVC7*-T^{152}D)	0.015
	TG1(pCR2.1-*qnrVC7*-T^{152}A)	0.25
QnrVC7, C^{172}	TG1(pCR2.1-*qnrVC7*-C^{172}T)	0.06
	TG1(pCR2.1-*qnrVC7*-C^{172}G)	0.015
	TG1(pCR2.1-*qnrVC7*-C^{172}L)	0.25
	TG1(pCR2.1-*qnrVC7*-C^{172}D)	0.015
	TG1(pCR2.1-*qnrVC7*-C^{172}A)	0.06
Double mutations	TG1(pCR2.1-*qnrVC7*-T^{152}A/Q^{132}L)	0.25
	TG1(pCR2.1-*qnrVC7*-T^{152}A/C^{172}L)	0.25
QnrVC5	TG1(pCR2.1-*qnrVC5*-Q^{132}L)	0.25
	TG1(pCR2.1-*qnrVC5*-C^{172}L)	0.25

[a] Strains TG1 and TG1(pCR2.1) denote the *E. coli* host strain and the corresponding strain harboring the pCR2.1 vector, respectively. The amino acid change of the respective protein is depicted in the strain identification (ID).
[b] CIP, ciprofloxacin.

QnrVC7. For residues A^{82} and A^{102}, all substitutions, including those with Gly, completely abolished its protective activity, with an exception being A^{102}S, which exhibited minor effects (Table 1). These data suggest that Ala, Ser, and, in some cases, Thr, were the best fitting residues at the i^{-2} position of face 4 on coils 1 to 4, and that the bulky side chain residues, such as Leu and Asp, would disrupt the well-organized tight stacks of these coils. The requirement for small side chain residues at the i^{-2} position was consistent with the finding in other Qnr proteins, such as QnrA and QnrC (11). However, substitution with Gly was not tolerated either, suggesting that the small side chain is required for forming the stable stack between coils. The best-fitting residues in these well-organized structure were also observable in the i^{-2} positions

proteins through enhancement of its protective activity to the same level as that exhibited by the other Qnr proteins. However, other substitutions, including $T^{152}G$, $T^{152}L$, and $T^{152}D$, completely abolished its protective activity. Structural analysis showed that the stack formed by coils 5 and 6 was a tight structure similar to that formed by coils 1 to 4; therefore, the rule for best-fitting residues also applies to this stack, in which the amino acid Ala or Ser was the best-fitting residue for maintenance of the stack structures of QnrVC7 and other Qnr proteins. Surprisingly, an i^{-2} residue of face 4 on coil 5, Q^{132}, was found to exhibit different functional properties. The amino acid substitutions $Q^{132}T$ and $Q^{132}G$ had no effect on the protective function of the protein, whereas the $Q^{132}D$ change completely abolished its activity. On the other hand, the $Q^{132}A$ and $Q^{132}L$ changes increased QnrVC7-protective strength by 2- and 4-fold, respectively, almost reaching the full capacity exhibited by the other Qnr proteins. Similarly, the reduced protective strength of QnrVC7 due to the T^{152} substitution could also be complemented through the $C^{172}L$ change at the i^{-2} position of face 4 on coil 7, presumably through interaction with residue F^{154} of QnrVC7 to stabilize the stack formed by coils 6 and 7 and coils 7 and 8. However, the stack formed by coils 7 and 8 was similar to other stacks, in that the amino acid substitutions $C^{172}A$ and $C^{172}T$ had no effect on QnrVC7-protective activity, whereas the $C^{172}D$ and $C^{172}G$ changes completely abolished such activity. These findings suggest that the protective effects of the stacks formed by coils 6 and 7 and coils 7 and 8 could be increased by enhancing the hydrophobic nature of residue on i^{-2} of face 4; for example, the $C^{172}L$ and $Q^{132}L$ substitutions could complement the less-optimal protective effect due to residue T^{152} in QnrVC7.

To further characterize the effects of different substitutions of residues in the i^{-2} position of face 4, double-amino acid substitutions ($T^{152}A/Q^{132}L$ and $T^{152}A/C^{172}L$) were introduced but were found to exhibit no further improvement in the QnrVC7 functions. In addition, the $Q^{312}L$ or $C^{712}L$ change created in QnrVC5 was found to exhibit a full protective effect but no further functional improvement. These data suggest that most Qnr proteins already exhibited full protective activity in their natural form, and that any reduction in protective activity due to amino acid substitutions in the i^{-2} position of coil 6, 7, or 8 could be readily reversed by the introduction of a hydrophobic residue, such as Leu.

Integrated analysis of the findings from this study and currently available data has advanced our understanding of Qnr proteins in the following aspects. First, face 2 of the Qnr protein was found to be in a well-organized status, whereas face 4 could be separated into three parts, in which part 1 was formed by coils 10, 1, 2, 3, and 4, part 2 by coils 5, to 7, and part 3 by coils 8 and 9 (Fig. 1B). Parts 1 and 2 were separated by loop B, whereas part 3 comprised a less-ordered coil and a C-terminal helix. Second, residues at the i position from all four faces were hydrophobic residues facing the inside of the Qnr protein and were found to play a very important role in stabilizing the overall structure of the protein, accommodating only small side chain residues at the i^{-2} position in all four faces. Previous mutational analysis data showed that some residues in the i position could tolerate substitutions by Ala, such as $F^{25}A$, $F^{30}A$, $L^{35}A$, and $F^{40}A$, yet some were sensitive to these substitutions, such as $F^{56}A$, $F^{66}A$, $W^{166}A$, and $L^{176}A$ (3). Due to the space constraint of the i-position hydrophobic residues, only small side chain residues, such as Thr, Ala, Ser, or Cys, were allowed at the i^{-2} position, according to our data on the i^{-2} position of face 4 and data from previous studies (3, 9). Third, an exception

to this rule is that the i^{-2} position of face 4 in coils 5 and 7 is located at the interface of three different parts. Due to the insertion of loop B into the region between parts 1 and 2, the stack formed by coils 4 and 5 was much wider than other well-organized stacks formed by other coils. It should be noted that the i^{-2} position on coil 5 tolerated the residue Gln, Thr, or Gly but not Asp. Interestingly, residues of a hydrophobic nature, such as Leu, helped stabilize parts 1 and 2 of the protein. In the case of QnrVC7, its protective effect was reduced by the substitution $A^{152}T$. The substitution may cause a conformational change of QnrVC7, therefore affecting the correct docking of QnrVC7 into gyrase A. The substitution $Q^{312}L$ could complement such a reduction in protective activity by stabilizing coil 5. Similarly, due to the less-organized structure of coil 8, an amino acid substitution at the i^{-2} of coil 7, $C^{172}L$, also mediated strong hydrophobic interactions with residues in the i position, such as L^{149} and F^{154}, further stabilized the structure, and improved protective activity (Fig. 1C). The restoration of a higher protective activity of QnrVC7 by mutations $Q^{132}L$ and $C^{172}L$, with predicted tighter stacking between coils 5 and 6 and 6 and 7, possibly functions by a better positioning of loop B, which is required for gyrase to disrupt quinolone action (5, 15). In summary, this study characterized a series of residues in the i^{-2} position of face 4 of QnrVC7 and demonstrated their role in stabilizing the structure of Qnr proteins for the maintenance of proper functions of such proteins, which advanced our understanding of the structure-activity relationship of Qnr proteins.

REFERENCES

1. **Vetting MW, Hegde SS, Wang M, Jacoby GA, Hooper DC, Blanchard JS.** 2011. Structure of QnrB1, a plasmid-mediated fluoroquinolone resistance factor. J Biol Chem **286**:25265–25273. http://dx.doi.org/10.1074/jbc.M111.226936.

2. **Hegde SS, Vetting MW, Roderick SL, Mitchenall LA, Maxwell A, Takiff HE, Blanchard JS.** 2005. A fluoroquinolone resistance protein from *Mycobacterium tuberculosis* that mimics DNA. Science **308**:1480–1483. http://dx.doi.org/10.1126/science.1110699.

3. **Jacoby GA, Corcoran MA, Mills DM, Griffin CM, Hooper DC.** 2013. Mutational analysis of quinolone resistance protein QnrB1. Antimicrob Agents Chemother **57**:5733–5736. http://dx.doi.org/10.1128/AAC.01533-13.

4. **Lahey Clinic.** 2015. *qnr* numbering and sequence. Lahey Clinic, Burlington, MA. http://www.lahey.org/qnrstudies/.

5. **Xiong X, Bromley EH, Oelschlaeger P, Woolfson DN, Spencer J.** 2011. Structural insights into quinolone antibiotic resistance mediated by pentapeptide repeat proteins: conserved surface loops direct the activity of a Qnr protein from a Gram-negative bacterium. Nucleic Acids Res **39**:3917–3927. http://dx.doi.org/10.1093/nar/gkq1296.

6. **Kim HB, Wang M, Ahmed S, Park CH, LaRocque RC, Faruque AS, Salam MA, Khan WA, Qadri F, Calderwood SB, Jacoby GA, Hooper DC.** 2010. Transferable quinolone resistance in *Vibrio cholerae*. Antimicrob Agents Chemother **54**:799–803. http://dx.doi.org/10.1128/AAC.01045-09.

7. **Fonseca ÉL, dos Santos Freitas F, Vieira VV, Vicente ACP.** 2008. New

qnr gene cassettes associated with superintegron repeats in *Vibrio cholerae* O1. Emerg Infect Dis **14:**1129–1131. http://dx.doi.org/10.3201/eid1407 .080132.

8. **Hegde SS, Vetting MW, Mitchenall LA, Maxwell A, Blanchard JS.** 2011. Structural and biochemical analysis of the pentapeptide repeat protein EfsQnr, a potent DNA gyrase inhibitor. Antimicrob Agents Chemother **55:**110–117. http://dx.doi.org/10.1128/AAC.01158-10.

9. **Rodríguez-Martínez JM, Briales A, Velasco C, Conejo MC, Martínez-Martínez L, Pascual A.** 2009. Mutational analysis of quinolone resistance in the plasmid-encoded pentapeptide repeat proteins QnrA, QnrB and QnrS. J Antimicrob Chemother **63:**1128–1134. http://dx.doi.org/10.1093 /jac/dkp111.

10. **Cattoir V, Poirel L, Nordmann P.** 2007. *In-vitro* mutagenesis of *qnrA* and *qnrS* genes and quinolone resistance in *Escherichia coli*. Clin Microbiol Infect **13:**940–943. http://dx.doi.org/10.1111/j.1469-0691.2007.01778.x.

11. **Guo Q, Weng J, Xu X, Wang M, Wang X, Ye X, Wang W, Wang M.** 2010. A mutational analysis and molecular dynamics simulation of quin-

olone resistance proteins QnrA1 and QnrC from *Proteus mirabilis*. BMC Struct Biol **10:**33. http://dx.doi.org/10.1186/1472-6807-10-33.

12. **Po KH, Wong MH, Chen S.** 2015. Identification and characterisation of a novel plasmid-mediated quinolone resistance gene, *qnrVC7*, in *Vibrio cholerae* of seafood origin. Int J Antimicrob Agents **45:**667–668. http://dx .doi.org/10.1016/j.ijantimicag.2015.02.002.

13. **Clinical and Laboratory Standards Institute.** 2010. Methods for antimicrobial dilution and disk susceptibility testing of infrequently isolated or fastidious bacteria; approved guideline, 2nd ed. CLSI document M45-A2. Clinical and Laboratory Standards Institute, Wayne, PA.

14. **Guo J, Chen S.** 2013. Unique substrate recognition mechanism of the botulinum neurotoxin D light chain. J Biol Chem **288:**27881–27887. http: //dx.doi.org/10.1074/jbc.M113.491134.

15. **Kim ES, Chen C, Braun M, Kim HY, Okumura R, Wang Y, Jacoby GA, Hooper DC.** 2015. Interactions between QnrB, QnrB mutants, and DNA gyrase. Antimicrob Agents Chemother **59:**5413–5419. http://dx.doi.org /10.1128/AAC.00771-15.